Proceedings of the 21st ICSMGE, Vienna, Austria, 14 – 19 June 2026. Pistrol, Adam & Schweiger (eds.)
Published by: ÖGG, Austrian Society for Geomechanics, Salzburg, Austria, ISBN 978-3-9503898-4-5
https://doi.org/10.53243/ICSMGE2026-1848

Geotechnical response of large diameter monopiles subjected to ship collision

K. A. Abhinav & L. Kellezi
Geo, Copenhagen, Denmark, aka@geo.dk

ABSTRACT: Offshore wind farms (OWFs) operate under the risk of collision from vessels due to their close proximity to international and domestic shipping lanes. Ship collision can result in significant downtime for the turbine or in the worst case, a total loss of the structure. Monopiles are the most common support structures for offshore wind turbines (OWTs) and have progressively grown in size to over 10 m in diameter. Major factors that dictate the outcome of a ship collision incident are – the position and velocity of impact, the kinetic energy of the ship and the properties of the supporting soil strata. Ship collision studies of are often performed by assuming the OWT to be clamped at its base, without considering the flexibility of the underlying soil. The presence of soil typically increases the deformations at the mudline, absorbing part of the energy from the ship's impact. Therefore, this study investigates the soil-structure interaction (SSI) of 6 m and 10 m diameter monopiles supporting conceptual 5 MW and 22 MW OWTs, within a finite element (FE) framework. Different vessel types and velocities are analyzed. The lateral response of the monopile is observed to be governed by a combination of factors – ship mass and velocity, monopile dimensions and soil stiffness along the depth. Results indicate that collisions at vessel speeds as low as 5 m/s, can result in unsafe lateral displacements (> 10% of the monopile diameter) of the OWT.

KEYWORDS: Offshore wind turbines (OWT), monopiles, ship collision, soil-structure interaction (SSI).

1 INTRODUCTION

The size of offshore wind turbines (OWTs) continues to increase, with installations extending into deeper waters and harsher environments. OWT structures are vulnerable to allision damage from vessels (commercial ships, maintenance craft, fishing trawlers etc.) passing nearby, at high speeds. Such allisions (where a moving vessel collides with a stationary object, such as an OWT monopile), though low in occurrence frequency, can result in injury to onboard personnel, production outage, environmental pollution and damage to turbine and vessel. In the present work, the terms collision and allision have been used interchangeably. With the rapid expansion of offshore wind energy infrastructure, the likelihood of vessel-structure interactions - including collisions involving both commercial shipping and service vessels - is expected to rise, underscoring the need for a better understanding of how these structures respond to impacts (Weigell and Jahn, 2022, Ma *et al.*, 2024).

In April 2020, *Njord Forseti*, a crew transfer vessel hit a monopile in the Borkum Riffgrund 1 offshore wind farm (OWF) in Germany, resulting in injuries to its crew (Thorrington, 2020). In January 2022, a bulk carrier *Julietta D* drifted into the Hollandse Kust Zuid OWF, damaging an under construction monopile and a jacket supporting a transformer platform (TM, 2023). In April 2023, the multipurpose vessel *PETRA L* collided with a turbine in the Gode Wind 1 OWF in the German North Sea, resulting in significant damage to the vessel (BSU, 2025). In August 2024, one crew member was confirmed dead and another reported missing, when the *ZD Yuyun*, a fishing vessel, struck an OWT in the Qidong H1 OWF off the Chinese coast in the Yellow Sea (Wright, 2025). In September 2024, a service vessel, Wind of Hope, allided with a wind turbine in the Hornsea 1 OWF, resulting in damages to both vessel and turbine (Emanuel, 2024). Causes for such allisions with OWT (and offshore structures in general) can vary from mechanical failures (TM, 2023) to human factors such as the failure to post a proper lookout (Wright, 2025). The aforementioned recent incidents highlight the need for further research into accidental loading on OWTs, resulting from ship collisions.

Based on numerical analysis, Broersen (2020) developed an analytical method to estimate the maximum overturning moment at the tower base and the mudline during a ship allision event. Bruun (2021) investigated the global response of a monopile OWT subjected to a ship collision by accounting for local deformations. Ladeira *et al.* (2023) presented a comprehensive literature review of the numerical, analytical and experimental methods for evaluating ship allision scenarios involving OWTs. Literature on OWT-ship allision events that consider soil-structure interaction (SSI) is limited. Samsonovs *et al* (2014) observed that while it does not influence the overall collapse behavior of an OWT, SSI modifies the structural response by introducing additional deformations at the base of the OWT.

This paper attempts to underscore the importance of considering SSI in the ship collision modelling of OWT by analyzing two different monopiles and soil profiles in the context of accidental loading within a finite element (FE) framework. Section 2 describes the FE approach used in the modelling and analysis. The bow collision model is elaborated in Section 3. Results are discussed in Section 4 and the paper concludes with Section 5.

2 NUMERICAL MODELLING

2.1 *Offshore reference wind turbines (RWTs)*

Two monopiles of different diameters – 6 m and 10 m - are considered in this study. They are assumed to support the NREL-5MW (Jonkman *et al.*, 2009) and the IEA Wind 22-MW (Zahle *et al.*, 2024) RWTs respectively. RWTs are commonly used by researchers for benchmarking studies in wind energy technology. The main properties of the two offshore RWTs and their support structures are summarized in Table 1.

Table 1. Properties of the reference wind turbines.

Parameter	NREL 5-MW	IEA Wind 22-MW
Rated power (MW)	5	22
Control	Variable speed, collective pitch	
Cut-in wind speed (m/s)	3	3
Rated wind speed (m/s)	11.4	11
Cut-out wind speed (m/s)	25	25
Rotor diameter (m)	126	284
Hub height (m)	90	170
Nacelle mass (t)	240	821.2
Tower mass (t)	347.5	1,574
Pile penetration (m)	36	45

The NREL-5MW and the IEA Wind 22-MW offshore RWTs are installed in water depths of 20 m and 34 m, respectively.

2.2 *Geotechnical model*

The FE program PLAXIS3D (Bentley, 2024a) has been used for geotechnical modelling of the offshore monopile. Initially, a validation exercise for ascertaining the suitability of PLAXIS3D for modelling monopile-soil interaction was conducted by comparison with previous studies by Kellezi & Abhinav (2025), Augustesen *et al.* (2010), Kellezi and Hansen (2003, 2002). Here, the FE program ABAQUS 3D (Hibbitt, Karlsson and Sorensen, 2002) and finite difference program FLAC 3D (Itasca, 2006) was used to analyze the lateral load response of a monopile of 4 m diameter in layered sandy soil, under an extreme mudline static load – bending moment combination of 4.6 MN and 95 MNm, along with the Winkler approach proposed by API (1993). As shown in Figure 1a & 1b, PLAXIS3D closely replicates the lateral displacement at pile top and depth-displacement curve obtained using ABAQUS 3D and FLAC 3D, respectively.

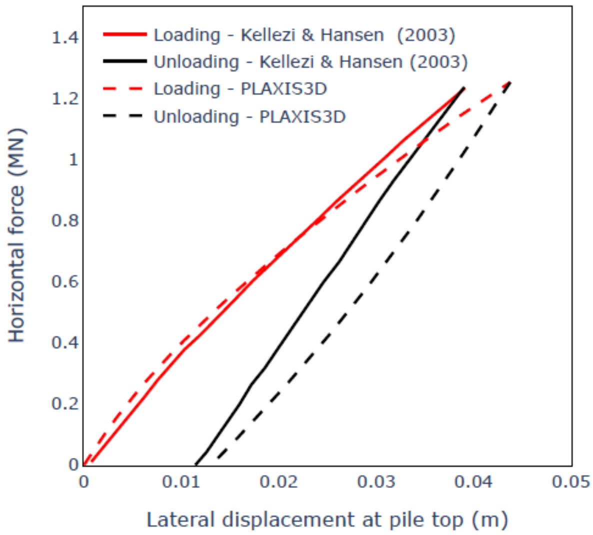

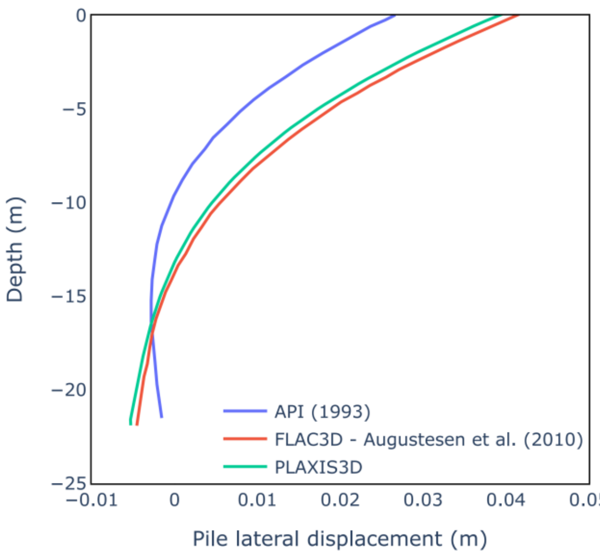

Figure 1. 1a-Top (Kellezi & Abhinav 2025) & 1b-bottom - Validation of PLAXIS monopile model

Owing to symmetry of the problem, only one half of the monopile is modelled in PLAXIS3D. The monopile structure is made up of linear-elastic isotropic shell/plate elements (Bentley, 2024b). The soil behavior was simulated with an elastoplastic model based on the Mohr-Coulomb failure criterion. The monopile is assumed to be wished-in-place and installation effects are ignored. The monopile is considered to be weightless, as this study focuses on lateral loading.

The interaction between the monopile and the soil continuum is simulated by means of interface elements. Node pairs, with one each belonging to the monopile and the soil, are generated at the interface. The relative displacement (slipping and gapping) between these two nodes are governed by two elastic-perfectly plastic springs. The shear and stiffness properties of the interface springs are dependent on the stiffness characteristics of the corresponding soil material (Bentley, 2024a).

The length of the model in the X and Y directions are 12 and 4 times the diameter of the monopile, respectively. A refined mesh zone is generated, extending to 0.20 times the diameter outside the circumference of the monopile and 0.15 times the diameter below the toe of the monopile (Bentley, 2024b). Dummy beams are inserted along the vertical edges of the monopile, in the FE model, for ease of post-processing. The dummy beams have a reduced stiffness such that the results are not influenced by their presence. The lateral displacements along the center-line of the monopile are obtained as the average of the displacements along the dummy beams. A FE model of the monopile in PLAXIS3D with dimensions is shown in Figure 2.

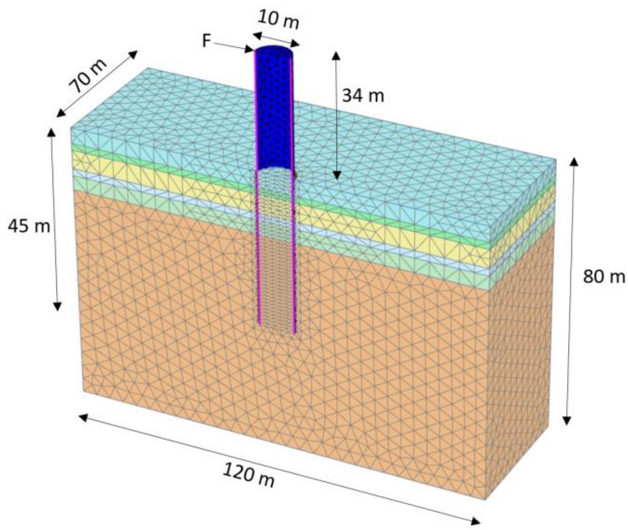

Figure 2. Finite element (FE) monopile model in PLAXIS3D

2.3 *Soil properties*

Two soil profiles are considered in this study. The first is uniformly sandy (Shen *et al.*, 2023) and is hereafter referred to, as Soil Profile A. The parameters used in the PLAXIS3D model are given in Table 2. Here, E_s is the secant Young's modulus, γ is the unit weight of soil and ϕ is the angle of internal friction.

Table 2. Soil Profile A

Soil type	Depth (m)	E_s (MPa)	γ (kN/m^3)	ϕ (°)
Sand	0 - 70	120	20	39

The second profile (referred to as Soil Profile B), in Table 3, comprises of layered sand, representative of the site conditions at the Horns Rev OWF. The soil properties, characterized by high values of peak friction angles has been re-interpreted from Kellezi & Hansen (2003, 2002) and Augustesen *et al.* (2010).

Table 3. Soil Profile B.

Soil type	Depth (m)	E_s (MPa)	γ (kN/m³)	ϕ (°)
Sand	0 – 4.5	84	20	42
Sand	4.5 – 6.5	51	20	40
Sand (silty)	6.5 – 11.9	46	20	37
Sand (silty)	11.9 – 14.0	36	20	35
Sand (silty/org.)	14.0 – 18.2	9	17	26
Sand	18.2 – 70.0	64	20	38

3 BOW COLLISION MODEL

During a collision event involving a vessel and a bottom fixed OWT structure, the energy transfer can be generalized as follows (Ladeira *et al.*, 2023):

$$K_0 = U_{ship} + U_{owt} + K_{ship} + K_{owt} + E_{hydro} + E_{soil} \quad (1)$$

Here, K_0 is the vessel's initial kinetic energy, U_{ship} and U_{owt} are the structural internal energies of the ship and the OWT, K_{ship} and K_{owt} are the kinetic energies after the collision, E_{hydro} and E_{soil} are the energy dissipated by hydrodynamic forces and SSI, respectively. Offshore design regulations (DNV GL, 2017) suggest the use of nonlinear dynamic FE analysis or simple elastic-plastic methods coupled with energy considerations for treating ship collisions from a structural point of view. However, the present work studies the response of large diameter monopiles under varying soil conditions, making use of a static load approach. Considering that the primary objective of this paper is to highlight the significance of incorporating SSI in ship collision studies, empirical models have been employed to effectively address the challenges associated with dynamic analysis limitations.

Pedersen *et al.* (1993) proposed a formulation to calculate the bow collision loads for merchant vessels between 500 deadweight tonnage (DWT) and 300000 DWT, as follows:

$$P_{bow} = \begin{cases} P_0\overline{L}\left[\overline{E}_{imp} + (5.0 - \overline{L})\overline{L}^{1.6}\right]^{0.5} & \text{if } \overline{E}_{imp} \geq \overline{L}^{2.6} \\ 2.24P_0\left[\overline{E}_{imp}\overline{L}\right]^{0.5} & \text{if } \overline{E}_{imp} < \overline{L}^{2.6} \end{cases} \quad (2)$$

where:

$\overline{L} = L_{pp}/275$ m

$\overline{E}_{imp} = E_{imp}/1425$ MNm

$E_{imp} = \frac{1}{2}m_x V_0^2$ MNm

Further, P_{bow} is the maximum bow collision load (MN), P_0 is the reference collision load (= 210 MN), E_{imp} is the energy absorbed by plastic deformations (MNm), L_{pp} is the length of the vessel (m), m_x is the mass plus added mass (10^6 kg) and V_0 is the initial speed of the vessel (m/s).

A typical offshore support vessel (OSV) like the VOS Stone (VOS, 2022) is considered in this study. These vessels support offshore operations including crew transfer, supplying water, fuel and other essentials to both oil & gas and offshore wind industries. The important structural features of the VOS Stone are given in Table 3.

The bow of the offshore support vessel is assumed to strike the OWT monopile, at the water surface. Two values are used for the vessel speed at collision – 2 m/s and 5 m/s. While deriving the bow collision loads, an added mass equal to 5% of the vessel mass is taken into account (Pedersen *et al.*, 1993). A schematic representation of bow collision with an OWT is shown in Figure 3.

Table 4. Specifications of offshore support vessel VOS Stone.

Parameter	Value
Length overall	80 m
Length between perpendiculars (L_{pp})	74.70 m
Maximum draught	5.8 m
Lightship	3313 t
Maximum displacement	4563 t
Maximum speed	13.3 kn

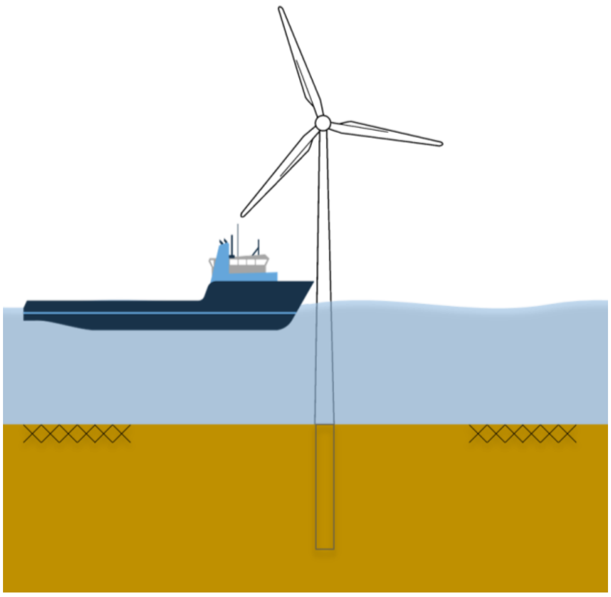

Figure 3. Bow collision with OWT

4 RESULTS

The FE calculations for the monopile lateral load analysis are performed in three stages. The soil properties are defined in the first stage. The pile is 'wished in place' without considering any installation effects, in the second stage and the lateral load is applied to its full capacity in the third. The lateral collision load applied at the water surface also generates a corresponding moment at the mudline, with lever arm equal to the water depth. A typical plot of the horizontal model deformations in PLAXIS3D is shown in Figure 4.

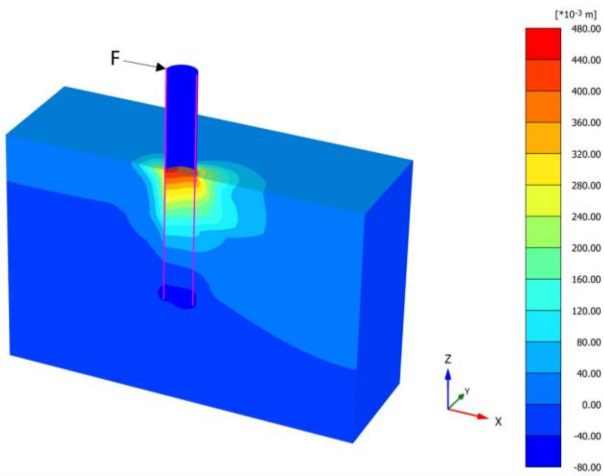

Figure 4. Horizontal model deformations in PLAXIS3D

4.1 *Pile lateral displacement*

The lateral displacement profiles of the 6 m diameter monopile supporting the NREL 5-MW OWT in Soil Profiles A and B are shown in Figures 5 and 6 respectively.

For both soil profiles, there is an increase in mudline lateral displacement to the tune of 60%, when the velocity of the vessel rises from 2 m/s to 5 m/s. For the pile toe-kick, this value is around 78%.

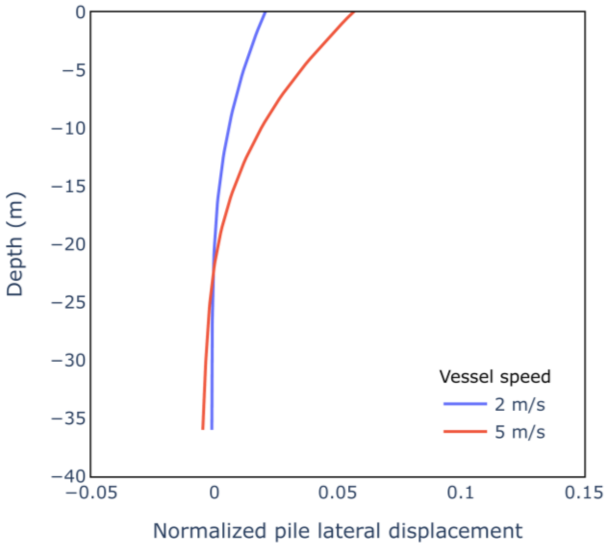

Figure 5. Lateral displacement profile – Soil profile A – 6 m dia.

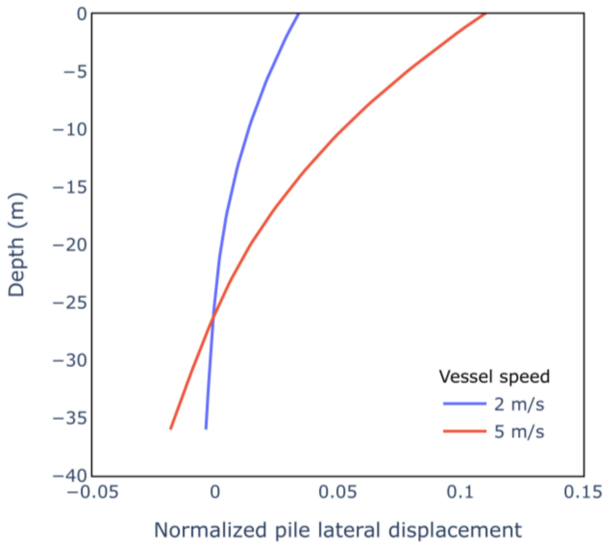

Figure 6. Lateral displacement profile – Soil profile B – 6 m dia.

Laterally loaded monopiles are considered to fail, when the mudline horizontal displacement exceeds 10% of the pile diameter (Bentley, 2024b). It can be observed from Figure 6 that for the 6 m diameter monopile this condition is attained, for a vessel speed of 5 m/s. However, this is not likely to be a critical situation as at this displacement magnitude, the failure mechanism is generally considered to be only partially developed (Bentley, 2024b). Further, in reality, consideration of vertical loads from the turbine and superstructure will result in increased soil stiffness and resistance (Li *et al.*, 2022).

Lateral displacement along the depth for the 10 m diameter monopile of the IEA Wind 22-MW OWT are plotted in Figures 7 and 8 respectively. For both soil profiles, there is an increase in mudline lateral displacement to the tune of 60%, when the velocity of the vessel rises from 2 m/s to 5 m/s. For the pile toe-displacement, this value is around 70%. It may be noted that lateral displacement is negligible near the toe region of the monopiles.

For both monopile diameters and vessel speeds, Soil Profile B consistently produces slightly higher lateral displacements than Soil Profile A, despite the presence of stiffer upper layers in Profile B. This behaviour can be attributed to the softer intermediate and deeper sand layers in Profile B, which govern the overall lateral stiffness once the load is transmitted beyond the initial embedment depth. While the stiff upper strata provide some resistance at small deflections, the deeper, more compliant layers allow greater pile rotation and deflection under the high bending moments generated during collision loading.

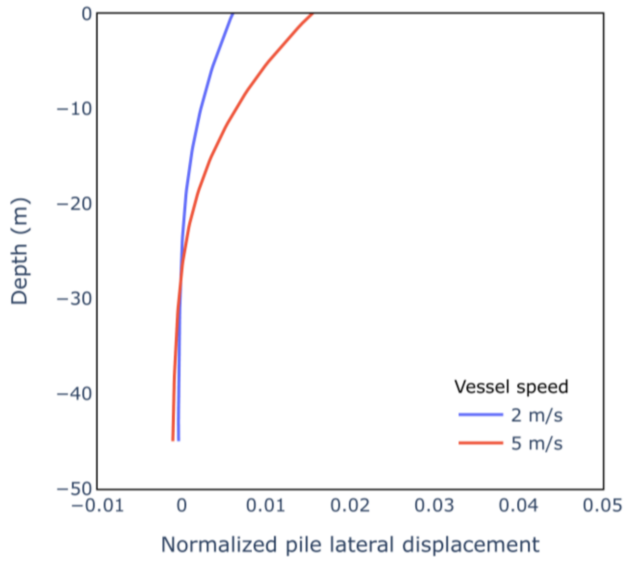

Figure 7. Lateral displacement profile – Soil profile A – 10 m dia.

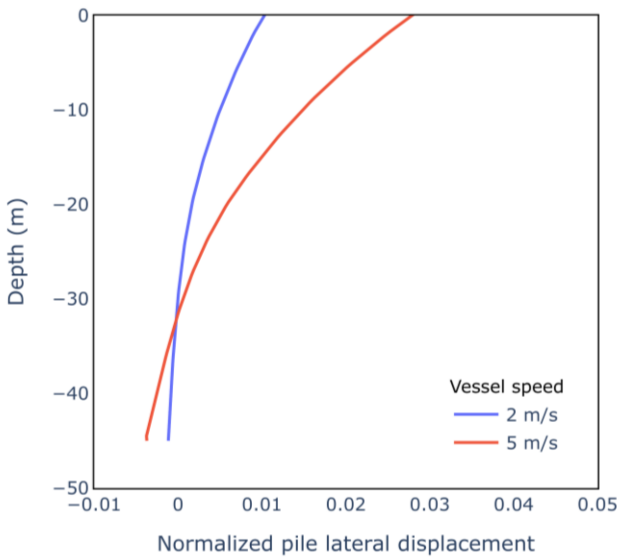

Figure 8. Lateral displacement profile – Soil profile B – 10 m dia.

4.2 *Influence of vessel type*

As seen in Equation (2), the mass and length between perpendiculars of the ship has a significant influence on the bow collision load. The influence of vessel dimensions and mass on the allision response of the IEA Wind 22-MW OWT monopile has been investigated with respect to two velocities at impact – 2 m/s and 5 m/s. Three different vessels – a coaster (HVR, 2024), an offshore supply vessel (VOS, 2022) and an icebreaker (Artica, 2014), as given in Table 5 are considered herein for the analysis.

Table 5. Vessel specifications.

Name	Type	L_{pp} (m)	Mass (t)
Unnamed	Coaster	77.40	2853
VOS Stone	Supply vessel	74.40	5463
MSV Fennica	Icebreaker	96.70	12800

The bow collision loads for the different vessels, computed for velocities of 2 m/s and 5 m/s, using Equation (2) are given in Table 6.

Table 6. Bow collision loads

Vessel Type ↓	Collision load at water surface (MN) ↓	
Velocity →	2 m/s	5 m/s
Coaster	16	40
Supply vessel	22	45
Icebreaker	37	73

Mudline pile displacement for the 10 m diameter monopile supporting the IEA Wind 22-MW OWT, under allision loads from three different vessels at varying velocities are plotted in Figures 9 and 10.

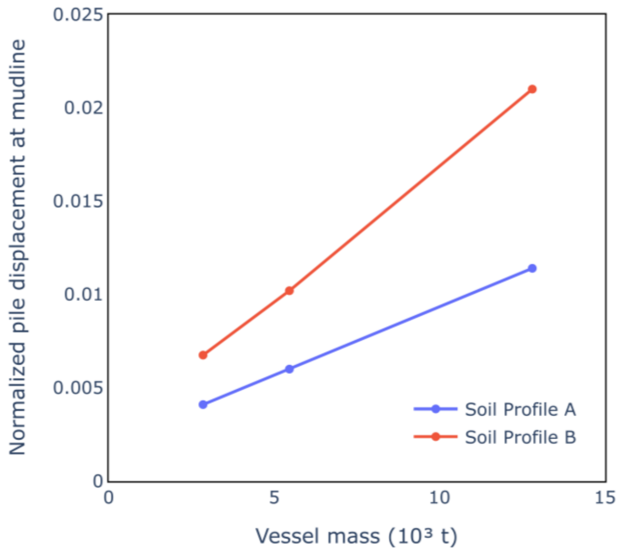

Figure 9. Displacement variation with vessel mass – 2 m/s

A clear interplay of the influence of vessel mass, dimensions, velocity and soil stiffness can be observed. Heavier vessels, such as the icebreaker are able to cause significant damage even at lower velocities. These observations underscore the importance of considering the full range of potential vessel types and operational scenarios when designing and constructing OWT structures, particularly with respect to ensuring that the monopile can withstand the maximum anticipated accidental lateral loads under various soil conditions.

Figures 11 and 12 show the variation of the lateral displacement of the 10 m diameter monopile at the mudline, with respect to the L_{pp} of the vessels. It may be noted that the mass of the vessel has a significantly higher bearing on the monopile displacement, than the L_{pp}. For instance, going from the coaster to the supply vessel, the displacement increases with mass, although there is a corresponding reduction in the L_{pp}.

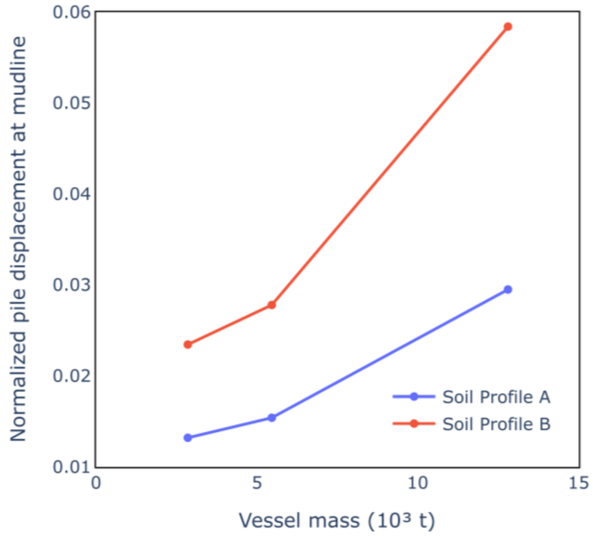

Figure 10. Displacement variation with vessel mass – 5 m/s

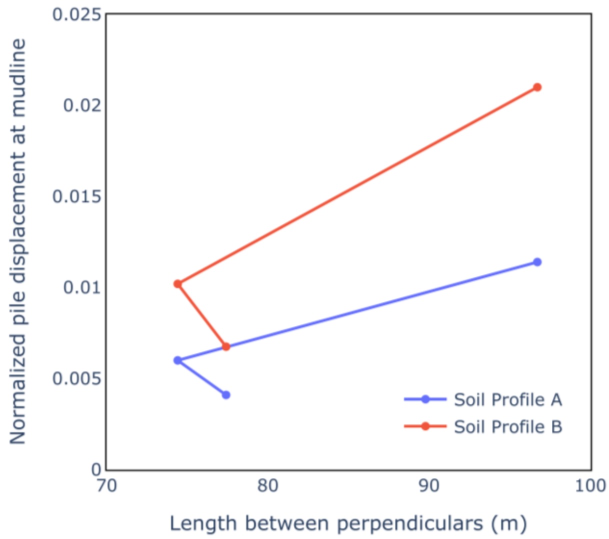

Figure 11. Displacement variation with vessel L_{pp} – 2 m/s

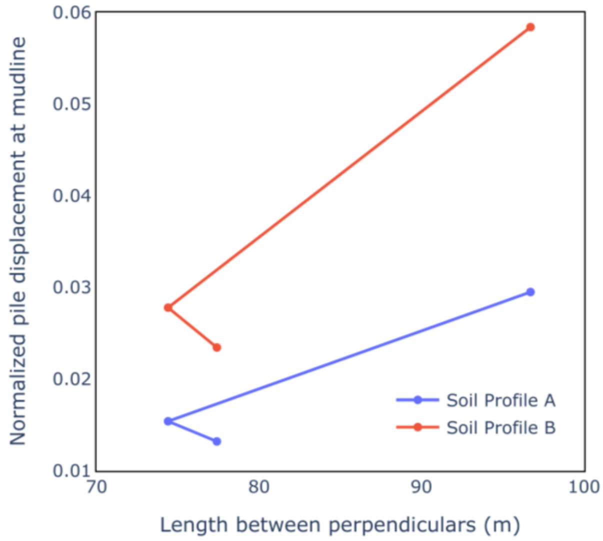

Figure 12. Displacement variation with vessel L_{pp} – 5 m/s

5 CONCLUSION

This study highlights the significance of accounting for soil-structure interaction (SSI) in the finite element (FE) analysis of ship collisions with offshore wind turbine (OWT) monopiles. Two different monopiles of 6 m and 10 m diameter are considered along with two different soil profiles – one uniform sand and the other, a realistic layered profile from an existing offshore wind farm (OWF). In weaker soils, it is observed that at speeds as low as 5 m/s, allisions can result in unsafe lateral displacements (> 10% of the monopile diameter). Lower soil stiffness at subsurface layers are noted to contribute significantly to the overall monopile lateral displacement and rotation. Lastly, the importance of considering a wide range of potential vessel types for design against accidental collision loading is highlighted.

The paper takes into account only the lateral load arising from the collision of the bow of a vessel, with a monopile supporting an OWT. The monopile in itself is considered to be weightless and the self-weight acting vertically is ignored, to investigate the effect of the lateral load on the structure. Further, a simple pseudo-static load model is adopted. An integrated model, considering the weight of the superstructure, including the turbine and the lateral loads from wind and wave along with impact loading from ship collision has been envisaged as part of future work.

6 ACKNOWLEDGEMENTS

The authors would like to thank Geo for financially supporting the preparation of this paper.

7 REFERENCES

API. 1993. *RP2A-WSD: Recommended practicefor planning, designing and constructing fixed offshore platforms – working stress design.* American Petroleum Institute.

Artica. 2014. MSV Fennica – short vessel description. Artica Offshore.

Augustesen, A. H., Sørensen, S. P. H., Ibsen, L. B., Andersen, L., Møller, M. and Brødbæk, K. T. 2010. Comparison of calculation approaches for monopiles for offshore wind turbines. *Numerical Methods in Geotechnical Engineering – Benz & Nordal (eds),* Taylor & Francis, 901-906.

Bentley. 2024a. Plaxis - Reference Manual 3D. Bentley Systems, Inc.

Bentley. 2024b. Plaxis - Monopile Designer Manual. Bentley Systems, Inc.

Broersen, A. M. 2020. Analytical model to assess bending moments in wind turbine support structures subjected to ship collisions. *Master's thesis*. Delft University of Technology and Norwegian University of Science and Technology.

Bruun, V. E. E. 2021. Ship collision analysis of monopile offshore wind turbines. *Master's thesis*. Norwegian University of Science and Technology.

BSU. 2025. *Allision with an offshore wind turbine in the Gode Wind 1 wind farm by the PETRA L on 24 April 2023 Investigation Report 192/23*. Bundesstelle für Seeunfalluntersuchung.

DNV GL. 2017. *RP –C204: Design against accidental loads*, DNV GL.

Emanuel, C. 2024. Service vessel "Wind of Hope" collides with turbine at Hornsea 1 wind farm. Available at: https://www.4coffshore.com/news/service-vessel-22wind-of-hope22-collides-with-turbine-at-hornsea-1-wind-farm-nid30341.html (Assessed: 11 August 2025).

Hibbitt, D., Karlsson, B. and Sorensen, P. 2002. ABAQUS/Standard User's Manual, Version 6.3. Providence, RI, USA: Dassault Systemes Simulia Corp.

HVR. 2024. *Investigation of ship impact against wind turbine foundations in the Dutch part of the North Sea*. Document No.: 081.R030.M006-Rev.4, HVR Engineering.

Itasca. 2006. FLAC3D Version 3.1. Itasca Consulting Group Inc.

Jonkman, J., Butterfield, S., Musial, W., and Scott G. 2009. Definition of a 5-MW Reference Wind Turbine for Offshore System Development, National Renewable Energy Laboratory, *Technical Report - NREL/TP-500-38060*.

Kellezi, L. and Abhinav, K. A. 2025. Soil Interaction Modelling of Large Diameter Offshore Wind Monopiles. *Engineering Materials, Structures, Systems and Methods for a More Sustainable Future, Proceedings Of the Ninth International Conference on Structural Engineering, Mechanics and Computation (SEMC 2025), Cape Town, South Africa, Zingoni, A. (Ed.)*. CRC Press, pp- 471-472.

Kellezi, L. and Hansen, P. 2003. Static and dynamic analysis of an offshore monopile windmill foundation. *Proceedings of BGA International Conference on Foundations, ICOF2003*, Dundee, Scotland, 2–5 Sept. 2003, pp.401–410. Thomas Telford Publishing.

Kellezi, L. and Hansen, P. 2002. Dynamic transient analysis of a monopile windmill foundation. EURODYN-2002, *Proceedings of the 4th International Conference on Structural Dynamics*, Munich, Germany, 2-5 Sept. 2002, pp. 1315‑1320.

Ladeira, I., Márquez, L., Echeverry, S., Le Sourne, H., and Rigo, P. 2023. Review of methods to assess the structural response of offshore wind turbines subjected to ship impacts. *Ships and Offshore Structures* 18(6), 755–774.

Li, Q., Gavin, K. G., Askarinejad, A., and Prendergast, L. J. 2022. Experimental and numerical investigation of the effect of vertical loading on the lateral behaviour of monopiles in sand. *Canadian Geotechnical Journal*, 59(5), 652-666.

Ma, L., Ding, J., Zhang, X., Wang, W., Zhao, X., Sun, C., and Yang, Y. 2024. Analysis of dynamic response of offshore wind turbines subjected to ship impacts and the corresponding protection measures: a review. *Frontiers in Energy Research* 12, 1497210.

Pedersen, P.T., Valsgaard, S., Olsen, D. and Spangenberg, S. 1993. Ship impacts: bow collisions. *International Journal of Impact Engineering*, 13(2), 163-187.

Samsonovs, A., Giuliani, L., and Zania, V. 2014. Soil structure interaction in offshore wind turbine collisions. *Proc. of the 9th International Conference on Structural Dynamics, EURODYN 2014*, Porto, 3651-3658.

Shen, J., Ge, C., Zhan, Y., Ye, Z., Zhang, Q., and Chen, J. 2023. Numerical Study on Lateral Response of Offshore Monopile in Sand under Local Scouring Conditions. *Journal of Marine Science and Engineering*, 11(1), 183.

Thorrington, D. A. 2020. Investigation into the causes of an allision between the windfarm support vessel Njord Forseti and a windfarm tower in the southern North Sea on 23rd April 2020. Jersey Maritime Administration.

TM. 2023. *Safety investigation into the loss of control of the Maltese registered bulk carrier JULIETTA D, Marine Safety Investigation Report No. 02/2023*. Transport Malta.

VOS. 2022. VOS Stone – Vessel particulars. Vroon. Accessed [05-08-2025].https://www.vroon.nl/uploads/vessels/Vessel-particulars/Vroon-Offshore-Services/VOS-Stone-vessel-particulars.pdf.

Wright, T. 2025. *Fishing Vessel Collision with China Wind Turbine Linked to Poor Lookout, Official Report Finds*. Available at: https://energymagz.com/35604/fishing-vessel-collision-with-china-wind-turbine-linked-to-poor-lookout-official-report-finds/ (Accessed: 11 August 2025).

Weigell, J., and Jahn, C. 2022. Assessing offshore wind farm collision risks using AIS data: An overview. In *Changing Tides: The New Role of Resilience and Sustainability in Logistics and Supply Chain Management–Innovative Approaches for the Shift to a New Era. Proceedings of the Hamburg International Conference of Logistics* (HICL), Vol. 33, pp. 499-521. Berlin.

Zahle, F., Barlas, A., Lønbæk, K., Bortolotti, P., Zalkind, D., Wang, L., Labuschagne, C., Sethuraman, L., and Barter, G. 2024. Definition of the IEA Wind 22-Megawatt Offshore Reference Wind Turbine. Technical University of Denmark, *DTU Wind Energy Report E-0243.*